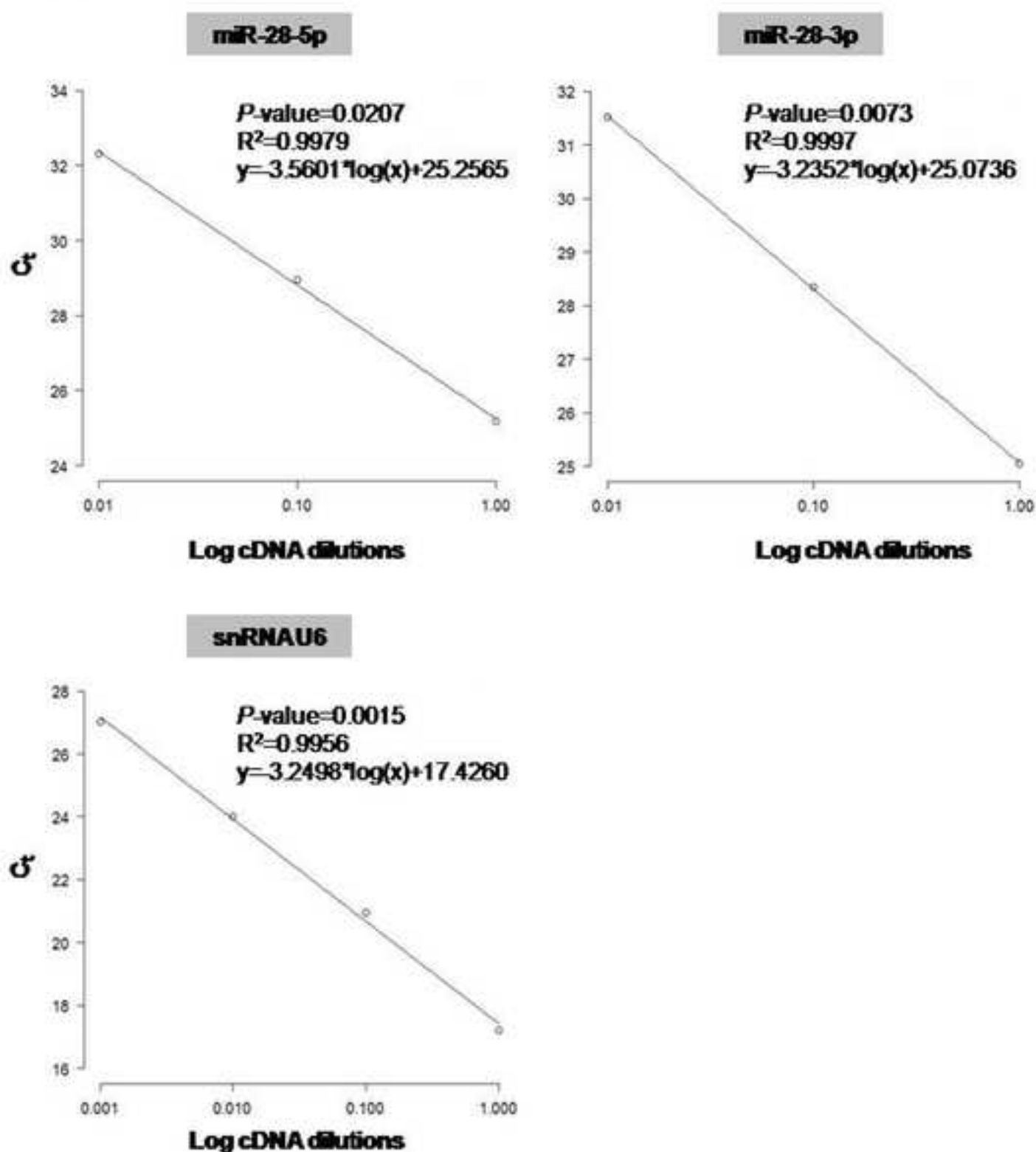
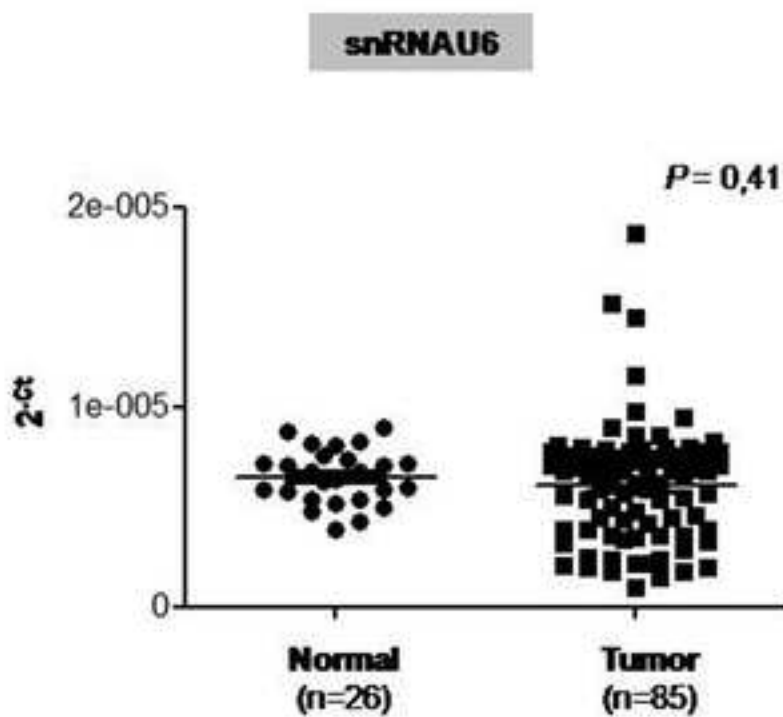


Supplementary Figure 1

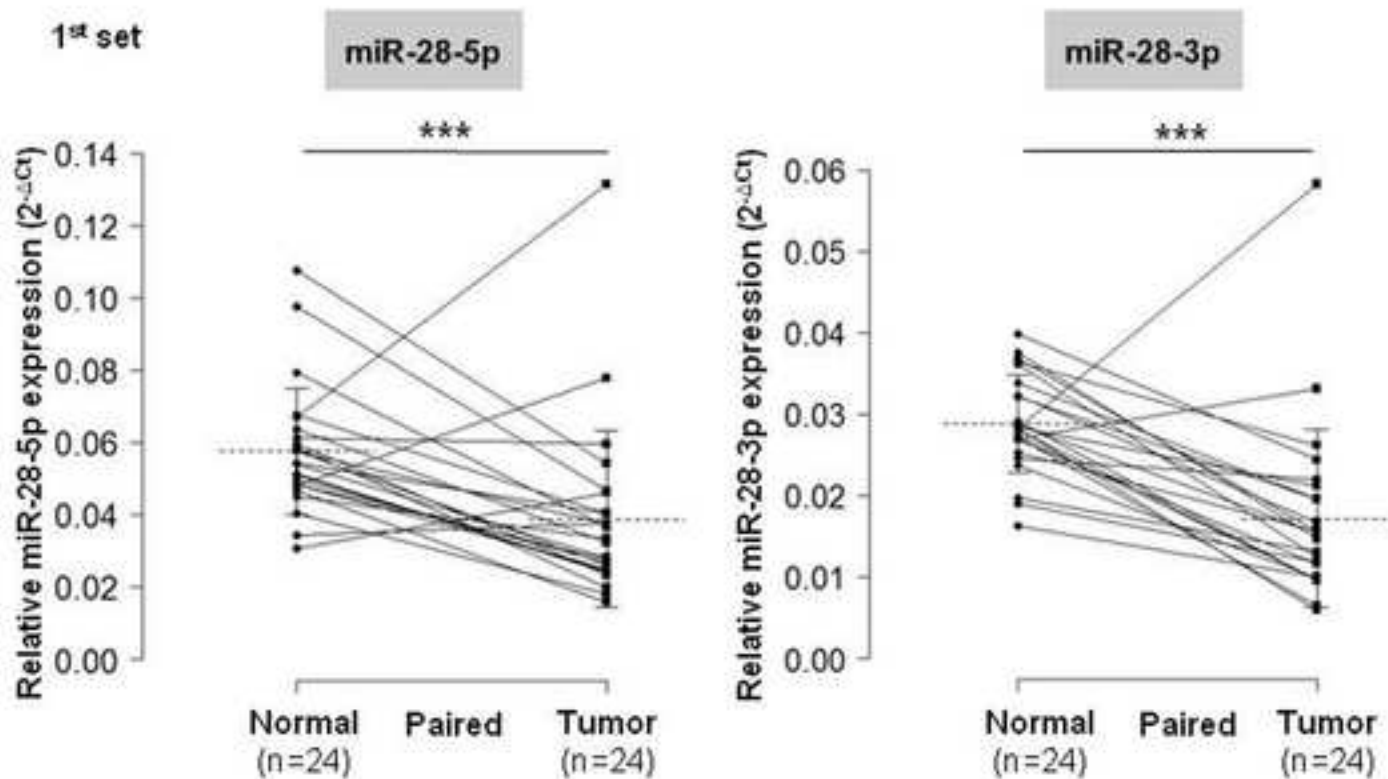
Supplementary Figure 1. Calibration curve determination of taqman assays for miR-28-5p, miR-28-3p and small nuclear RNA U6. Serial 10-fold dilutions of cDNA were amplified by quantitative real-time polymerase chain reaction. Equation and P values were determined using R software.

Supplementary Figure 2



Supplementary Figure 2. Evaluation of the reference gene small nuclear RNA U6 variations between samples from normal colon and tumor tissue. There are no differences in small nuclear RNA U6 (snRNA U6) expression between the two groups ($P=0,41$, Mann-Whitney-Wilcoxon test).

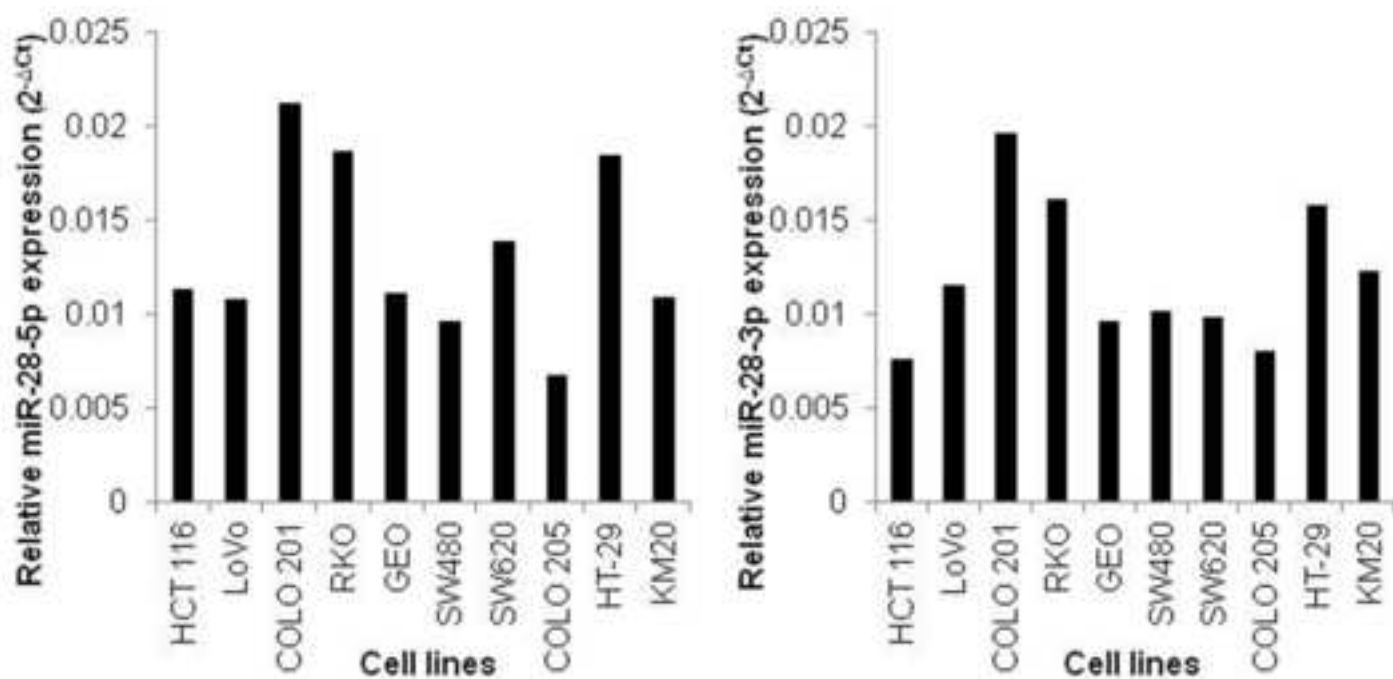
Supplementary Figure 3



Supplemental Figure 3. Twenty-four normal specimens from the first set of patients were paired with colon cancer tissues from the same patient. All values of miRNA expression levels were normalized by small nuclear RNA U6.

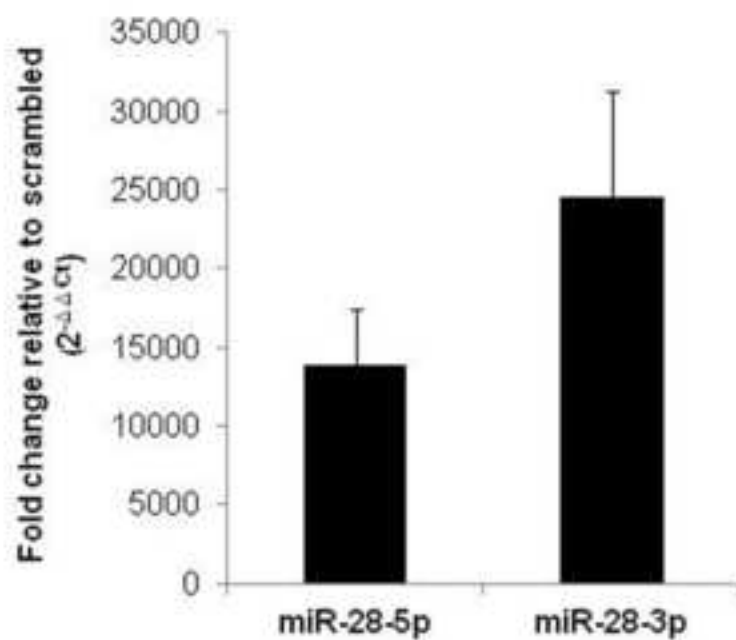
Significant differences were *** $P < 0.005$ using paired t test.

Supplementary Figure 4



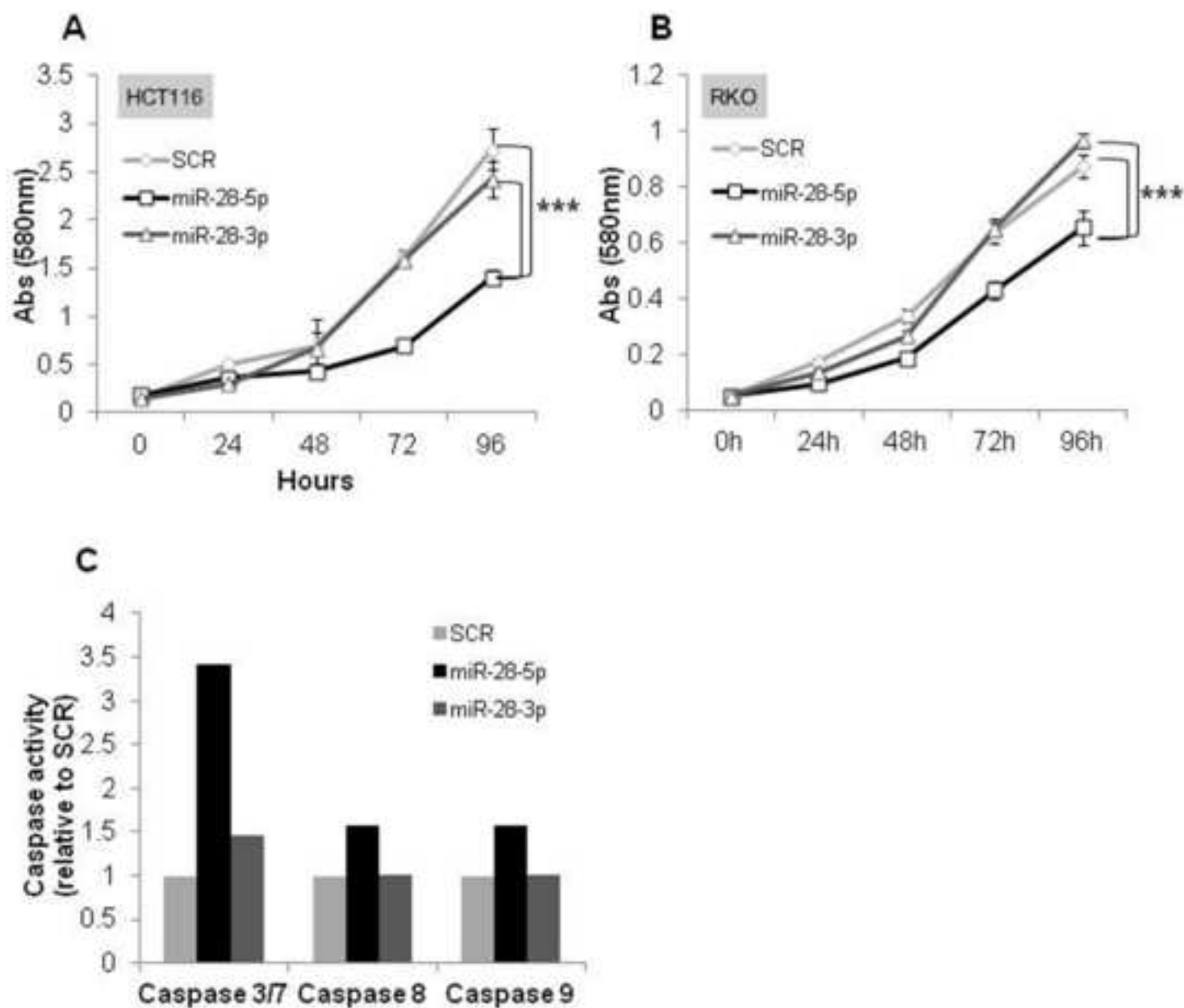
Supplemental Figure 4. Endogenous levels of miR-28-5p and miR-28-3p in 10 colon cancer cell lines. Small nuclear RNA U6 was used as a normalizer.

Supplementary Figure 5



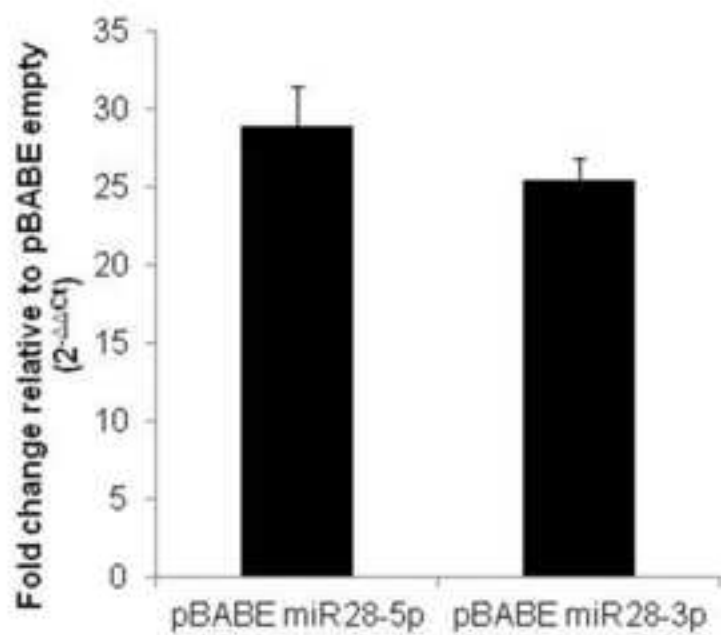
Supplementary Figure 5. miR-28-5p and miR-28-3p levels were measured by quantitative real time PCR after transient transfection of HCT116 cells with miR-28-5p and miR-28-3p precursors. Values were normalized to small nuclear RNA U6 and are representative of 2 independent experiments. Values shown are relative to negative control.

Supplementary Figure 6



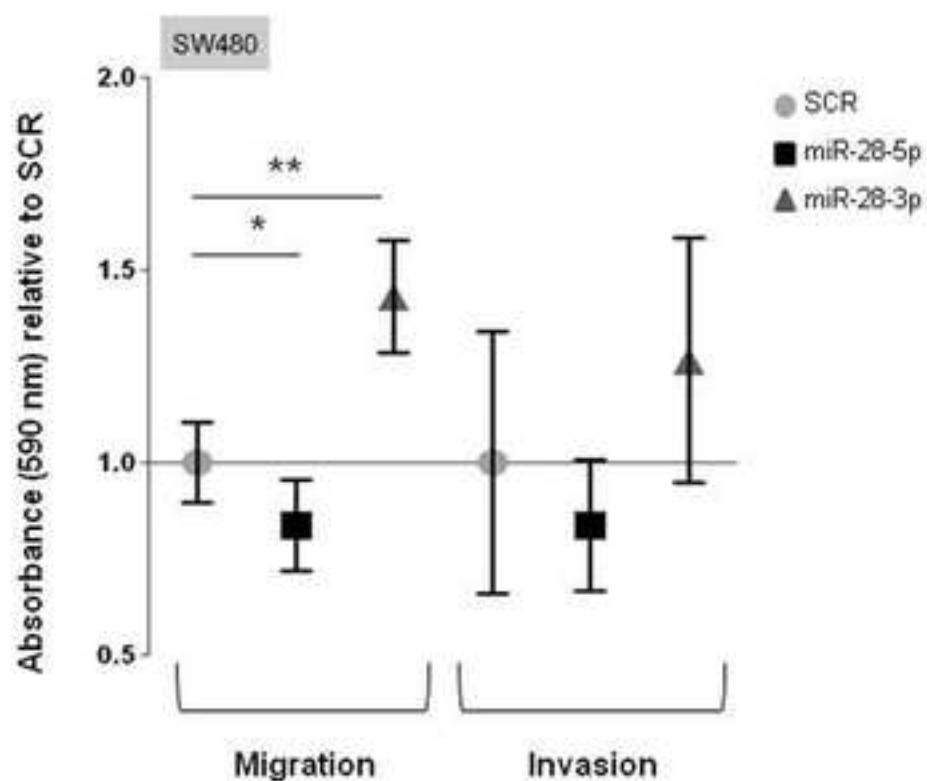
Supplemental Figure 6. MTT proliferation assay in (A) HCT116 and (B) RKO cell lines. miR-28-5p but not miR-28-3p inhibited cell growth compared with scrambled negative control (SCR). Values represent the average \pm SD of 8 replicates. (C) Caspase activity was measured in the HCT116 cell line 48 h after transfection with SCR (n=1), miR-28-5p, or miR-28-3p.

Supplementary Figure 7



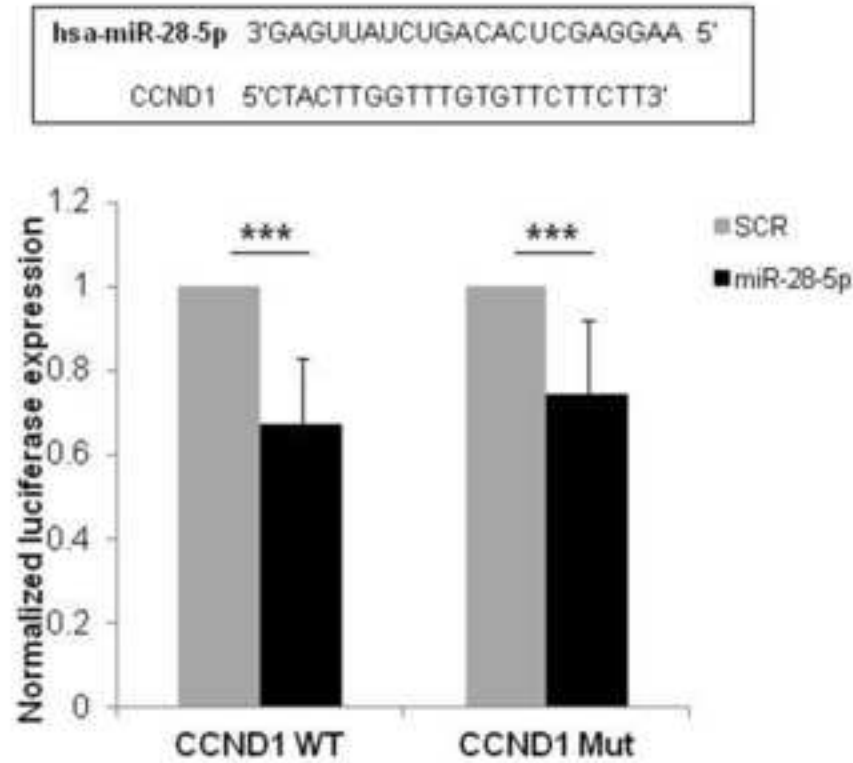
Supplemental Figure 7. miR-28-5p and miR-28-3p levels were measured by Real Time quantitative Reverse Transcription PCR after generating the stable clone pBabe-miR-28 in the HCT116 cell line. Values were normalized to small nuclear RNA U6 and are representative of 2 independent experiments. Values shown are relative to the control pBabe-empty vector.

Supplementary Figure 8



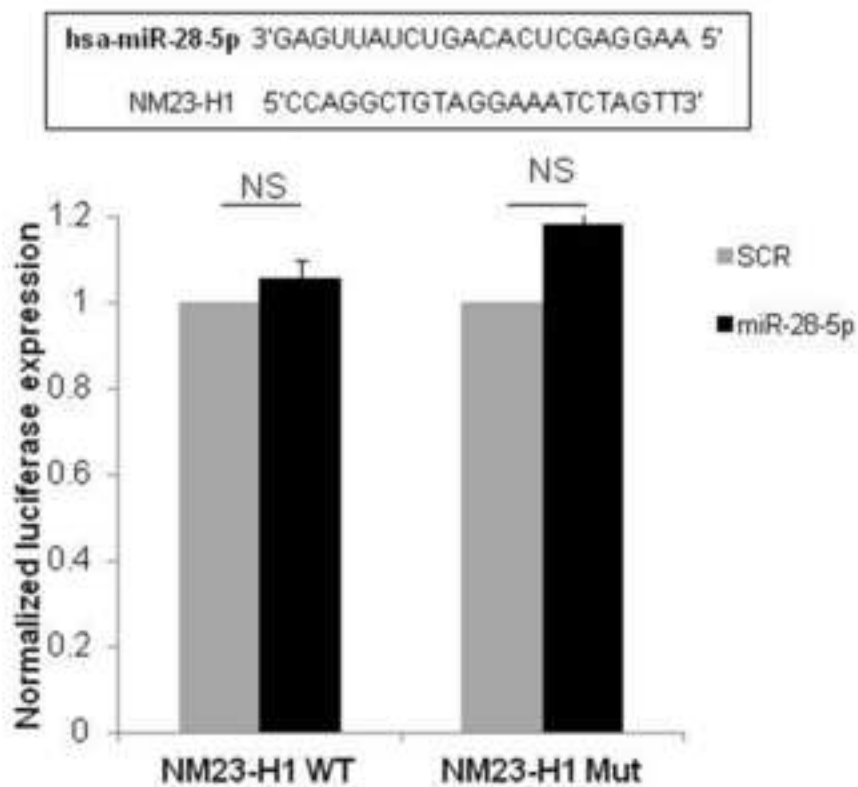
Supplementary Figure 8. Effect of miR-28-5p and miR-28-3p in migration and invasion in vitro in SW480 cell line. Absorbance was measured for cells on the bottom of noncoated and matrigel-coated transwell chambers at 24 h (for migration) and 48 h (for invasion) after SW480 cells expressing miR-28-5p or miR-28-3p were plated. Results are shown relative to scrambled negative control (SCR). A representative experiment is shown. Average (of triplicates) \pm standard deviation is shown (* $P < 0.05$, ** $P < 0.01$, Student *t* test).

Supplementary Figure 9



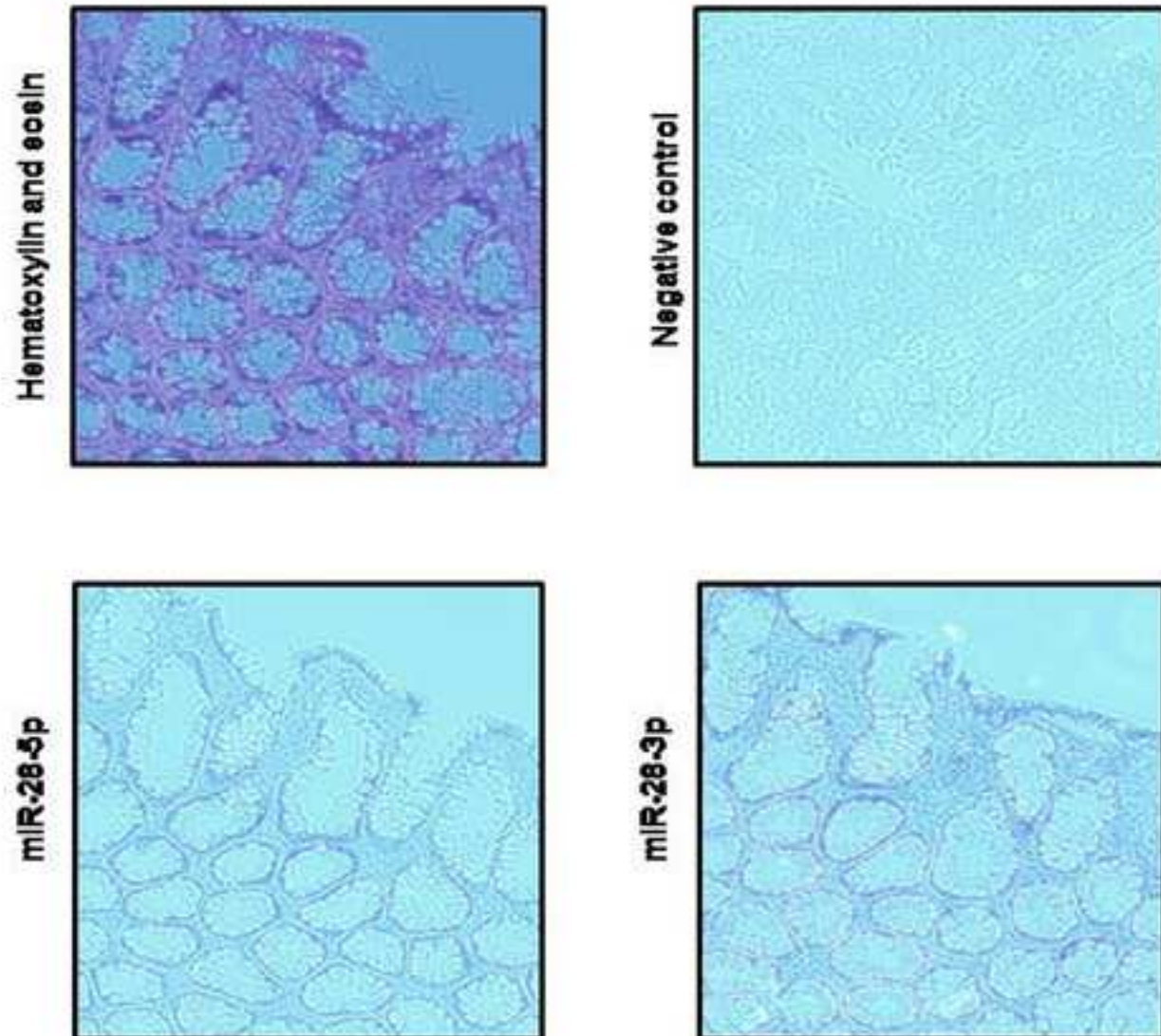
Supplemental Figure 9. Luciferase activity of HCT116 cells cotransfected with scrambled negative control (n=1) or miR-28-5p and PGL3-CCND1-WT. Experiment was also performed with a construct in which the binding site was mutated (** $P < 0.005$, Student *t* test).

Supplementary Figure 10



Supplementary Figure 10. Luciferase activity of HCT116 cells cotransfected with scrambled negative control (n=1) or miR-28-5p and PGL3-NM23-H1-WT. Experiment was also performed with a construct in which the binding site was mutated. NS: not statistical significant (Student *t* test).

Supplementary Figure 11



Supplementary Figure 11. *In situ* hybridization analysis for miR-28-5p and miR-28-3p in normal colon tissue. Frozen tissue sections were digested with proteinase K and loaded onto Ventan Discovery Ultra. The tissue slides were incubated with double-DIG labeled miRCURY LNA Detection probe and the digoxigenin was detected with a polyclonal anti-DIG antibody and UltraMap Blue anti-Ms Detection Kit. Hematoxylin and eosin staining was performed. Microscopy images were obtained with a magnification of 100X.

SUPPLEMENTARY MATERIAL

Strand-Specific miR-28-5p and miR-28-3p Have Distinct Effects in Colorectal Cancer Cells

Maria I. Almeida, Milena Nicoloso, Lizhi Zeng, Cristina Ivan, Riccardo Spizzo, Roberta Gafà, Lianchun Xiao, Xinna Zhang, Ivan Vannini, Francesca Fanini, Muller Fabbri, Giovanni Lanza, Rui M. Reis, Patrick A. Zweidler-McKay, and George A. Calin

Supplementary Methods

Microsatellite analysis

Microsatellite analysis was performed on DNA extracted from frozen tissue samples by a standard phenol-chloroform procedure. MSI was evaluated with a fluorescence based PCR method using the five markers of the Bethesda panel (D5S346, D17S250, D2S123, BAT25 and BAT26) plus BAT40. Analysis of PCR products was done with an automated DNA sequencer. Tumors were classified as MSS, MSI-L and MSI-H according to the guidelines of the International Workshop of Bethesda¹.

RNA and Protein Extraction

RNA was isolated using Trizol reagent (Invitrogen), according to the manufacturer's instructions. RNA quantity and purity was assessed with NanoDrop ND-1000 (Thermo Fisher Scientific, Wilmington, DE). RNA integrity was analyzed by gel electrophoresis. RNA samples were denatured at 70°C for 5 min, immediately placed on ice and loaded on an agarose gel stained with ethidium bromide. Intensity of the 18S and 28S bands was examined.

Total protein extracts were prepared in ice-cold lysis buffer (0.5% Nonidet P-40 [NP-40], 250 mM sodium chloride [NaCl], 50 mM *N*-2-hydroxyethylpiperazine-*N*-2-ethanesulfonic acid [Hepes], 5 mM ethylenediaminetetraacetic acid [EDTA], and 0.5 mM ethyleneglycol bis (beta-aminoethylether)-*N,N,N',N'* tetraacetic acid [EGTA]) containing phosphatase inhibitor cocktail 2 (Sigma-Aldrich, St. Louis, MO), protease inhibitor (Clontech, Mountain View, CA), and dithiothreitol (DTT) (Invitrogen, Carlsbad, CA).

Reverse Transcription - Quantitative Real-Time Polymerase Chain Reaction (RT-qPCR)

microRNAs expression was evaluated using TaqMan miRNA assays (Applied Biosystems, Foster City, CA). Briefly, complementary DNA (cDNA) was synthesized using RNA as a template, gene-specific stem-loop Reverse Transcription primer, and the TaqMan microRNA reverse-transcription kit (Applied Biosystems). Quantitative real-time PCR was carried out in a CFX384 real-time system (Bio-Rad, Hercules, CA) using cDNA, TaqMan probe, and TaqMan universal PCR master mix (Applied Biosystems). Experiments were performed in duplicate and normalized to small nuclear RNA U6, which was used as an internal control. Relative expression levels were calculated using the comparative cycle threshold (C_t) method. Stability of the reference gene between samples was analyzed. PCR efficiency was determined using the formula: Efficiency= $10^{-1/\text{slope}}-1$.

Cell Culture, STR DNA fingerprinting and miRNA Mimics Transfection

Human CRC HCT116, RKO and SW480 cell lines (purchased from American Type Culture Collection, Manassas, VA) were grown as suggested by the supplier. Cells were cultured at 37°C in 5% CO₂.

All cell lines used in this study were validated by STR DNA fingerprinting using the AmpF λ STR Identifier kit according to manufacturer instructions (Applied Biosystems). The STR profiles were compared to known ATCC fingerprints (ATCC.org), to the Cell Line Integrated Molecular Authentication database (CLIMA) version 0.1.200808 (<http://bioinformatics.istge.it/clima/>)² and to the MD Anderson fingerprint database. STR profiles of HCT116, RKO and SW480 cell lines matched known DNA fingerprints and were unique.

Pre-miRNA miRNA precursor molecules for hsa-miR-28-5p and hsa-miR-28-3p and Pre-miR miRNA precursor scrambled negative control #2 (SCR) were purchased from Ambion (Austin, TX). Transfections were performed using 50 nM of the miRNA specific-strand precursor molecules or control and Lipofectamine 2000 reagent (Invitrogen), according to the manufacturer's instructions. RNA and proteins were collected at 48 h after transfection. miRNA transfection efficiencies were evaluated by RT-qPCR.

MTT (3-(4,5-dimethylthiazol-2-yl)-2,5-diphenyltetrazolium bromide) assay

We seeded 5×10^3 HCT116 cells transfected with either scrambled negative control (SCR) or miR-28-5p in a 96-well plate, in 8 replicates for each condition. At each time point (0, 24, 48, 72 and 96 h post-transfection), the colorimetric reagent was added to the cells. After 2 h incubation at 37°C, dimethylsulfoxide (DMSO) was added. Proliferation was assessed by measuring absorbance at 580 nm using the SpectraMax Plus³⁸⁴ microplate reader (Molecular Devices, Sunnyvale, CA). Experiment was performed 2 times independently.

Apoptosis Quantification

Protein levels of the apoptotic molecular marker poly(adenosine diphosphate-ribose) polymerase 1 (PARP1), full length and cleavage PARP1 forms, were assessed by western blot analysis using PARP antibody (9542) from Cell Signaling Technology (Danvers, MA) in the HCT116 and RKO cell lines transfected with SCR, miR-28-5p, or miR-28-3p. Relative intensity of bands observed by western blotting was obtained using ImageJ software (<http://imagej.nih.gov/ij/>). In addition, caspase 3/7, 8, and 9 activity was measured.

Caspase 3/7, 8, and 9 Activity

Caspase activity was measured using Caspase-Glo 3/7 Assay Systems, Caspase-Glo 8 Assay Systems, and Caspase-Glo 9 Assay Systems (Promega Corporation) in HCT116 cells transfected with SCR, miR-28-5p, or miR-28-3p. The assay was performed 48 h posttransfection according to manufacturer' instructions, and luminescence was measured in a POLARstar OPTIMA microplate reader (BMG Labtech, Ortenberg, Germany).

Cell-Cycle Analysis by Flow Cytometry

For fluorescent-activated cell sorting (FACS) analysis, 6×10^5 HCT116 cells transfected with either SCR, miR-28-5p, or miR-28-3p were plated onto 6-well plates. After 48 h, cells were collected and fixed with 70% ice-cold ethanol. Cells were stained with a solution containing 0.05 mg/mL propidium iodide (Sigma-Aldrich) and 0.1 mg/mL RNase A (Roche, Indianapolis, IN) in phosphate-buffered saline. Cell-cycle

analysis was performed in a FACSCalibur flow cytometer (Becton Dickinson, San Jose, CA). The results were analyzed using ModFit LT software.

In Vitro Cell Migration and Invasion Assays

After 24- or 48-h incubation (for migration and invasion assay, respectively) at 37°C with 5% CO₂, cells were fixed with paraformaldehyde (USB Corporation, Cleveland, OH). Cells on the upper surface of the chamber (nonmigratory cells) were removed using cotton swabs, and cells on the bottom surface (migratory cells) were stained with crystal violet in 20% methanol for 20 min. Finally, 30% acetic acid was added to dissolve the crystal violet, and absorbance was measured in a SpectraMax Plus³⁸⁴ spectrophotometer (Molecular Devices) at 590 nm.

Establishment of miR-28-Expressing Cell Line: Cell Transduction with Retroviral Vector

A PCR fragment of 483 nt that included the human miR-28 precursor and flanking sequences was amplified using primers with BamHI and EcoRI endonucleases restriction sites (Supplementary Table 4). pBABE-puro retroviral plasmid and miR-28-containing fragment were digested with BamHI and EcoRI enzymes and ligated using T4 DNA ligase (New England Biolabs, Ipswich, MA). Constructs were checked by direct sequencing. The retroviral plasmid pBABE-miR28 was transiently transfected, together with pVSV-G vector, into GP2-293 cells using Lipofectamine 2000 reagent (Invitrogen). The retroviral plasmid pBABE-empty was used as a control. Cells were fed with fresh medium the day after transfection. Viral supernatant was collected 3 days after transfection, filtered through 0.45-µm pore, and supplemented with sequa-brene (Sigma-Aldrich). HCT116 cells (that are known to have metastatic potential³) were infected and selected using puromycin. Successful establishment of HCT116-pBABE-miR28 cell line was verified by RT-qPCR.

Cell Transduction with Lentiviral Vector

As pBABE-puro does not contain green fluorescent protein (GFP) marker and to facilitate the detection of the human colon cancer cells in the in vivo studies, HCT116-pBABE-empty and HCT116-pBABE-miR28 cells were transduced in parallel with empty pRRL-CMV-PGK-GFP-WPRE (Tween) lentiviral vector.

Briefly, pTween vector was cotransfected with the packaging vector pCMVDR8.74 and the envelope vector pMD.G into 293FT cells using Lipofectamine 2000 reagent (Invitrogen). Forty-eight hours after transfection, supernatant containing the virus was collected, filtered through 0.45- μ m pore, and supplemented with sequa-brene. HCT116-pBABE-empty and HCT116-pBABE-miR28 were incubated with the viral soup for 45 min while centrifuged at 32°C at 1800 rpm, plus another 1 h and 15 min in the incubator at 37°C. Infection efficiency was evaluated by flow cytometry by detecting the percentage of GFP-positive cells (>85%).

miRNA Target Prediction

We performed in silico analysis to determine miR-28-5p- and miR-28-3p-predicted targets using an in-house Perl script that scans the databases for the algorithms PITA (<http://genie.weizmann.ac.il/pubs/mir07>), TargetScan (<http://www.targetscan.org>), miRanda (<http://www.microrna.org>), and RNA22 (<http://cbcsrv.watson.ibm.com/>) for target identification. miR-28 sequence annotation was obtained from the miRBase database (<http://www.mirbase.org/>) (Supplementary Table 4).

Western Blot Analysis for miRNA Targets

Proteins were collected 48 h after cells were transfected with SCR, miR-28-5p, or miR-28-3p. Bradford assay was used to measure protein concentration. Proteins were separated by polyacrylamide gel (Bio-Rad) electrophoresis and were transferred to 0.2 μ m nitrocellulose membranes (Bio-Rad). The following antibodies were used: anti-CyclinD1 (sc-20044), anti-HoxB3 (sc-28606), and anti-Nm23-H1 (sc-343) all from Santa Cruz Biotechnology (Santa Cruz, CA). Proteins were detected by chemiluminescence. Anti-glyceraldehyde-3-phosphate dehydrogenase (GAPDH) from Cell Signaling Technology or anti-vinculin (sc-5573) from Santa Cruz Biotechnology were used as normalizers.

Luciferase Reporter Assays

Fragments of about 200 nt that contained the miR-28-5p and miR-28-3p putative binding sites were amplified by PCR using primers containing the XbaI restriction enzyme site (Supplementary Table 4).

PCR products were purified, digested, and directly cloned into the XbaI site of the pGL3 control vector (Promega Corporation, Madison, WI), located downstream of the firefly luciferase reporter gene. The QuikChange II XL site-directed mutagenesis kit (Agilent Technologies, Santa Clara, CA) was used to generate mutations in the miRNA-binding site (Supplementary Table 4).

HCT116 cells were seeded (1×10^5 cells/well) in 24-well plates. After 24 h, cells were cotransfected with 50 nM of SCR, miR-28-5p, or miR-28-3p and 0.4 μ g pGL3-putative binding site plasmids or pGL3-mutated putative binding site plasmids, together with Renilla luciferase construct that was used as a normalization reference. Transfections were performed in OPTI-MEM I (Invitrogen) using Lipofectamine 2000 reagent (Invitrogen). Cells were lysed 48 h after transfection, and luciferase activity was measured using a dual-luciferase reporter assay system (Promega Corporation) in the veritas microplate luminometer (Turner Biosystems). Two independent experiments were performed with 4 replicates each. Normalized relative luciferase activity was calculated by the formula: [Firefly luciferase]/[Renilla luciferase] activity. All constructs were confirmed by direct sequencing using an ABI 3730xl DNA analyzer sequencer (Applied Biosystems).

Supplementary Table 1. Efficiency of Taqman Assay for miR-28-5p (assay number 000411), miR-28-3p (assay number 002446) and snRNA U6 (assay number 001973) using the C_t slope method. PCR efficiency was determined using the formula: $\text{Efficiency} = 10^{-1/\text{slope}} - 1$.

Taqman Assay	R ²	Slope	Efficiency ($=10^{-1/\text{slope}} - 1$)
miR-28-5p	0.9979	-3.5601	0.91
miR-28-3p	0.9997	-3.2352	1.04
snRNA U6	0.9956	-3.2498	1.03

Supplementary Table 2. Mean values +/- standard error of the mean (SEM) of miRNA-28-5p and miR-28-3p expression (using ΔC_t method) in normal colon and colorectal cancer samples, for two independent sets. Values were normalized to small nuclear RNA U6.

			Mean	SEM
miR-28-5p	1st set of samples	Normal	0.058	0.003
		Tumor	0.044	0.003
		MSS	0.043	0.004
		MSI	0.046	0.004
	2nd set of samples	Normal	0.238	0.025
		Tumor	0.151	0.019
miR-28-3p	1st set of samples	Normal	0.029	0.001
		Tumor	0.022	0.002
		MSS	0.022	0.002
		MSI	0.022	0.002
	2nd set of samples	Normal	0.319	0.028
		Tumor	0.161	0.017

Supplementary Table 3. miR-28-5p expression in colorectal cancer comparing to normal colon in two independent sets of samples using Pfaffl method, REST 2009 Software (Qiagen, V2.0.13, <http://www.qiagen.com/Products/REST2009Software.aspx?r=8042#Tabs=t1>). Small nuclear RNA U6 was used as a reference gene.

Gene	Type	Reaction efficiency	Samples	Expression	Std. Error	95% C.I.	P(H1)	Result
miR-28-5p	Target	0,9094	1st set (paired)	0,620	0,389-0,971	0,258-2,380	0,000	Down
			2nd set (paired)	0,641	0,320-1,254	0,173-2,544	0,003	Down
			1st set (all)	0,711	0,441-1,209	0,211-2,282	0,001	Down
U6	Reference	1,0309		1				

Supplementary Table 4. Sequences of mature human miR-28-5p and miR-28-3p according to miRBase, primers used to amplify miR-28, and primers used to generate PGL3- constructs for luciferase assays and to generate deletions in the miRNA-binding site. Restriction sites for endonucleases are underlined.

Mature miRNA	Sequences
hsa-miR-28-5p	AAGGAGCUCACAGUCUAUUGAG
hsa-miR-28-3p	CACUAGAUUGUGAGCUCCUGGA
Primers	
mir-28-Fw-BamHI	<u>CGGATCC</u> AGGCCCTTCAAGGACTTTCT
miR-28-Rv-EcoRI	CGAATTCACAGAGCTCCTGCTGTGTCA
Primer for PGL3 construct	
CCND1_XbaI_Fw	CGTCTAGAGTCCCCTCCTACGATACGC
CCND1_XbaI_Rv	CGTCTAGACTTGCCTCAAAGTCCTGCTT
HOXB3_XbaI_Fw	CGTCTAGAAAGGACATTGTGTTTCCTGTCA
HOXB3_XbaI_Rv	CGTCTAGACAAAGAAAGTTCCAAGAGGGAAT
NM23_XbaI_Fw	CGTCTAGAGCAGACCACATTGCTTTTCA
NM23_XbaI_Rv	CGTCTAGAAACCAACTCAATGAATCCTATGC
Primers for mutagenesis	
CCND1 Mutagenesis Fw	GGTTCAACCCACAGCTACTTGCATATTCTAAAACCATCCAT
CCND1 Mutagenesis Rv	ATGGAATGGTTTTAGAAATATGCAAGTAGCTGTGGGTGAACC
HOXB3 Mutagenesis Fw	GTTCTAAAAGGCATGAACTCATCGTCACTGTATAGTCCTG
HOXB3 Mutagenesis Rv	CAGGACTATACAGTGACGATGAGTTCATGCCTTTTAGAAC
NM23 Mutagenesis Fw	AGAGGACCAGGCTGTAGGATATTTACAGGAACCTCATC
NM23 Mutagenesis Rv	GATGAAGTTCCTGTAAATATCCTACAGCCTGGTCTCT

Supplementary Figure Legends

Supplementary Figure 1. Calibration curve determination of Taqman assays for miR-28-5p, miR-28-3p and small nuclear RNA U6. Serial 10-fold dilutions of cDNA were amplified by quantitative real-time polymerase chain reaction. Equation and P values were determined using R software.

Supplementary Figure 2. Evaluation of the reference gene small nuclear RNA U6 (snRNA U6) variations between samples from normal colon and tumor tissue. There are no differences in small nuclear RNA U6 expression between the two groups ($P = 0,41$, Mann-Whitney-Wilcoxon test).

Supplementary Figure 3. Twenty-four normal specimens from the first set of patients were paired with colon cancer tissues from the same patient. All values of miRNA expression levels were normalized by small nuclear RNA U6. Significant differences were $^{***}P < 0.005$ using paired t test.

Supplementary Figure 4. Endogenous levels of miR-28-5p and miR-28-3p in 10 colon cancer cell lines. Small nuclear RNA U6 was used as a normalizer.

Supplementary Figure 5. miR-28-5p and miR-28-3p levels were measured by quantitative real time PCR after transient transfection of HCT116 cells with miR-28-5p and miR-28-3p precursors. Values were normalized to small nuclear RNA U6 and are representative of 2 independent experiments. Values shown are relative to negative control.

Supplemental Figure 6. MTT proliferation assay in (A) HCT116 and (B) RKO cell lines. miR-28-5p but not miR-28-3p inhibited cell growth compared with scrambled negative control (SCR). Values represent the average \pm SD of 8 replicates. (C) Caspase activity was measured in the HCT116 cell line 48 h after transfection with SCR ($n=1$), miR-28-5p, or miR-28-3p.

Supplementary Figure 7. miR-28-5p and miR-28-3p levels were measured by quantitative real time PCR after generating the stable clone pBabe-miR-28 in the HCT116 cell line. Values were normalized to small nuclear RNA U6 and are representative of 2 independent experiments. Values shown are relative to the control pBABE-empty (n=1).

Supplementary Figure 8. Effect of mir-28-5p and miR-28-3p in migration and invasion in vitro in SW480 cell line. Absorbance was measured for cells on the bottom of noncoated and matrigel-coated transwell chambers at 24 h (for migration) and 48 h (for invasion) after SW480 cells expressing miR-28-5p or miR-28-3p were plated. Results are shown relative to scrambled negative control (SCR). A representative experiment is shown. Average (of triplicates) +/- standard deviation is shown (* $P < 0.05$, ** $P < 0.01$, Student t test).

Supplementary Figure 9. Luciferase activity of HCT116 cells cotransfected with scrambled negative control (n=1) or miR-28-5p and PGL3-*CCND1*-WT. Experiment was also performed with a construct in which the binding site was mutated (** $P < 0.005$, Student t test).

Supplementary Figure 10. Luciferase activity of HCT116 cells cotransfected with scrambled negative control (n=1) or miR-28-5p and PGL3-*NM23-H1*-WT. Experiment was also performed with a construct in which the binding site was mutated. NS: not statistical significant (Student t test).

Supplementary Figure 11. In situ hybridization analysis for miR-28-5p and miR-28-3p in normal colon tissue. Frozen tissue sections were digested with proteinase K and loaded onto Ventan Discovery Ultra. The tissue slides were incubated with double-DIG labeled miRCURY LNA Detection probe and the digoxigenin was detected with a polyclonal anti-DIG antibody and UltraMap Blue anti-Ms Detection Kit. Hematoxylin and eosin staining was performed. Microscopy images were obtained with a magnification of 100X.

Supplementary References

1. Boland CR, Thibodeau SN, Hamilton SR, et al. A National Cancer Institute Workshop on Microsatellite Instability for cancer detection and familial predisposition: development of international criteria for the determination of microsatellite instability in colorectal cancer. *Cancer Res.* 1998;58(22):5248-57
2. Romano P, Manniello A, Aresu O, et al. Cell Line Data Base: structure and recent improvements towards molecular authentication of human cell lines. *Nucleic Acids Res.* 2009;37:D925-32.
3. Rajput A, Dominguez San Martin I, Rose R, et al. Characterization of HCT116 human colon cancer cells in an orthotopic model. *J Surg Res* 2008;147(2):276-81.